J. Fluid Mech. (2009), *vol.* 624, *pp.* 45–55.
doi:10.1017/S0022112008004473 Printed in the United Kingdom

Available potential energy diagnosis in a direct numerical simulation of rotating stratified turbulence

GUILLAUME ROULLET† AND PATRICE KLEIN

Laboratoire de Physique des Océans UMR6523 (CNRS, UBO, IFREMER, IRD), Brest, France

(Received 15 May 2008 and in revised form 4 October 2008)

Review of three studies devoted to the available potential energy (APE) leads to the proposal of a diagnosis for APE, well-suited for rotating stratified flows within the primitive equations (PE) framework in which anharmonic effects (due to large vertical displacements of isopycnals) are permitted. The chosen diagnosis is based on the APE definition of Holliday & McIntyre (*J. Fluid Mech.*, vol. 107, 1981, pp. 221–225) and uses the background stratification of Winters *et al.* (*J. Fluid Mech.*, vol. 289, 1995, pp. 115–128). Subsequent evaluation of the APE in a PE direct simulation ($1/100°$, 200 levels) of oceanic mesoscale turbulence indicates that anharmonic effects are significant. These effects are due to large vertical displacements of the isopycnals and the curvature of the background density profile.

1. Introduction

For quasi-geostrophic (QG) stratified rotating turbulent flows, characterized by small vertical displacements of isopycnals, Charney (1971) predicted that one third of the total energy would be in potential form, in accordance with the energy equipartition principle. Such equipartition has been confirmed in numerical simulations of three-dimensional QG turbulence (Hua & Haidvogel 1986; McWilliams 1989). In these flows the available potential energy (APE) diagnosis has a quadratic form based on the smallness of the isopycnal vertical displacements. There is no equivalent theory for the primitive equations (PE) framework which allows flow regimes with large vertical displacements of isopycnals. The potential energy is actually rarely used and in any case is never diagnosed in PE numerical simulations. This is because of the lack of an adequate APE diagnosis that would take into account the non-quadratic, or anharmonic, effects of APE, which require consideration of higher order terms. In this paper we review in § 2 some studies devoted to the definition of APE. Their synthesis allows us to propose a more accurate APE definition for the PE framework. Such diagnosis is used in § 3 to analyse APE properties, in particular anharmonic effects, in a PE direct numerical simulation (DNS). Conclusions are offered in the last section.

† Email address for correspondence: roullet@univ-brest.fr

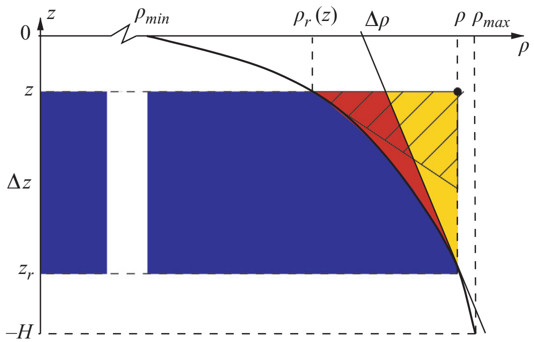

FIGURE 1. Graphical interpretation of the three APE densities in terms of areas, all based on a reference stratification $\rho_r(z)$ (thick line): Holliday & McIntyre's (1980) APE (2.1) of a parcel ρ at depth z is the sum of the yellow and red areas; the basic APE (2.2) for the same parcel is the sum of the blue, red and yellow areas; QG APE (2.5) is the yellow area, whereas QG APE (2.6) is the hatched area. Equation (2.5) is based on the slope of the reference profile $N_r^2(z_r)$ (thin straight line) and (2.6) on the slope of the profile at z. Anharmonic effects (taken into account in (2.1) and not in (2.5)) are shown by the red area.

2. A review of APE density

2.1. *The three definitions of APE density*

The potential energy of a fluid parcel with density $\rho(x, y, z, t)$ is $e_p(z, \rho) = \rho g z$ (with g being the gravity constant). This energy is never diagnosed because it is neither quadratic nor linear in the perturbation.

A better quantity to use is APE density proposed by Holliday & McIntyre (1981) that measures the potential energy with respect to a reference state:

$$e_a(z, \rho) = \int_{z_r(\rho)}^{z} g(\rho - \rho_r(z'))\,\mathrm{d}z', \tag{2.1}$$

where $\rho_r(z)$ is the density profile of this reference state and $z_r(\rho)$ is its inverse mapping. Physically, $z_r(\rho)$ is the equilibrium depth of a parcel of density ρ. Equation (2.1) includes two terms. The first one, $g\rho\Delta z$ (where $\Delta z = z - z_r(\rho)$ is the vertical displacement of the isopycnals), is the work of the gravitational force (see Holliday & McIntyre 1981), and the second, $\int_{z_r(\rho)}^{z} \rho_r(z')g\,\mathrm{d}z'$, is the work of the pressure force due to the background stratification. A graphical interpretation of this APE is given in figure 1 as the sum of the red and yellow areas. It is actually the area delimited by the curve $z_r(\rho)$ and the horizontal and vertical lines emanating from the point (z, ρ). This APE definition requires no assumption on Δz. One important constraint for this definition is that $z_r(\rho)$ must exist for any ρ value present in the fluid, and therefore the reference state should span the interval from ρ_{min} to ρ_{max}. As noted by Holliday & McIntyre (1981), this APE density is not quadratic in the perturbation because it includes higher order corrections, namely anharmonic terms, but it has the essential property of being definite positive as long as the reference profile is stable.

A more basic expression for APE density is

$$e_W(z, \rho) = g\rho\Delta z \tag{2.2}$$

that retains only the gravitational force term of (2.1). It was used by Winters *et al.* (1995) to obtain volume-integrated APE. This basic APE is the sum of the blue, red and yellow areas in figure 1. If $\rho_b(z)$ is a volume-preserving rearrangement of $\rho(x, y, z)$

(as in Winters *et al.* 1995), then the two APEs yield the same domain integrated value:

$$E_a[\rho] = \int_V e_a(z, \rho(x, y, z, t))\,\mathrm{d}V = \int_V e_W(z, \rho(x, y, z, t))\,\mathrm{d}V. \tag{2.3}$$

However, if one is interested in the local APE density, then only (2.1) is valid because the additional work of the pressure force (blue area in figure 1), at leading order in Δz, cancels out the gravitational force (the sum of red, yellow and blue areas in figure 1) and transforms the linear form (2.2) into the definite positive form (2.1) while preserving (2.3). The Hamiltonian approach (§ 2.2) provides the unifying framework.

A further simpler and classical expression for APE is the one that uses, for a fixed density, a Taylor series expansion of (2.1) in $\Delta z = z - z_r(\rho)$ (assuming the smallness of Δz), that is

$$e_a(z, \rho) = -g\left(\frac{1}{2}\partial_z\rho_r\Delta z^2 + \frac{1}{6}\partial^2_{zz}\rho_r\Delta z^3\right) + O(\Delta z^4). \tag{2.4}$$

The second-order term involves the density gradient and the third-order one the curvature of the reference density profile. If only the second-order term is retained (2.4) yields the QG APE density (Pedlosky 1987) that is quadratic and reads

$$e_{QG}(z, \rho) = \frac{1}{2}\rho_0\left[N_r(z_r)\Delta z\right]^2, \tag{2.5}$$

where ρ_0 is the constant density associated with the Boussinesq assumption, and $N_r^2(z_r) = -\rho_0^{-1}g\partial_z\rho_r(z_r)$ is the square of the Brunt–Väisälä frequency of the reference stratification. The right triangle approximating the QG APE is the yellow area in figure 1 in which the hypotenuse is given by the local slope $N_r^2(z_r)$ of the profile. Equation (2.1) turns out to be the finite amplitude form of (2.5) and therefore a more accurate definition of APE when Δz is large. Conversely, expanding (2.1) in Δz, at fixed z, yields the QG APE density written for the density perturbation $\Delta\rho = \rho - \rho_r(z)$:

$$e^*_{QG}(z, \rho) = \frac{1}{2}\rho_0\left[\frac{g\Delta\rho}{\rho_0 N_r(z)}\right]^2 \tag{2.6}$$

(hatched right triangle in figure 1). For a non-uniform reference profile (2.5) and (2.6) differ. In particular, the slopes of the triangles are different. Equation (2.5) is associated with the Lagrangian view (fixed ρ), whereas (2.6), the most customary, is associated with the Eulerian view (fixed z).

We define the anharmonic effect by

$$e_{anh}(z, \rho) = e_a(z, \rho) - e_{QG}(z, \rho) \tag{2.7}$$

(red area in figure 1); at leading order in Δz it is proportional to Δz^3 and the curvature of the reference profile $\partial^2_{zz}\rho_r$ (see (2.4) and (2.5)). Using e^*_{QG} instead of e_{QG} in (2.7) would give an anharmonic effect with opposite sign and a slightly different magnitude.

The choice of (2.1) was validated by Shepherd (1993) and Bannon (2003) who furthermore explored the role of the pressure forces with the help of the Hamiltonian formalism as described in § 2.2. Then the only question to address is the choice of the reference stratification. This point is discussed in §§ 2.3 and 2.4. The next issue will be to determine how (2.5) differs from (2.1) in a highly ageostrophic regime that exhibits large isopycnal deviations and therefore to quantify the importance of the anharmonic effects. These effects, shown by the red area in figure 1, are quantified in § 3.

2.2. *Hamiltonian formalism*

We follow in this section some ideas developed in Shepherd (1993) to better understand the role of the pressure force. Prior to the APE definition, two density functionals are introduced: the total potential energy

$$E_p[\rho] = \int_V \rho(x, y, z, t) g z \, \mathrm{d}V \tag{2.8}$$

and a Casimir which, for a rest state, reduces to a functional of the density

$$C[\rho] = \int_V f_r(\rho) \, \mathrm{d}V, \tag{2.9}$$

where $f_r(\rho)$ is a function defined on the reference state (see Morrison 1998 for a good introduction on Hamiltonian fluid dynamics). This Casimir is chosen to cancel the linear contributions in the perturbation. The total APE then reads

$$E_a[\rho] = E_p[\rho] - E_p[\rho_r] + C[\rho] - C[\rho_r], \tag{2.10}$$

which is also called the potential part of the pseudo-energy. In order for the Casimir to have no impact on the global form of energy, i.e. $C[\rho] = C[\rho_r]$, $\rho_r(z)$ must be a volume-preserving rearrangement of $\rho(x, y, z)$. This sets a strong constraint on the reference profile. In this case, the introduction of the Casimir only modifies the APE local form. Shepherd (1993) gives an extensive review of various APEs associated with various sets of fluid dynamics equations. Applied to the case of stratified rotating incompressible flows, hydrostatic or not, the Casimir reads

$$f_r(\rho) = -p_r(z_r(\rho)) - \rho g z_r(\rho), \tag{2.11}$$

where $p_r(z)$ is the hydrostatic pressure associated with the reference stratification. Hence, APE density reads

$$e_a(z, \rho) = \rho g z - \rho g z_r(\rho) - p_r(z_r(\rho)) + p_r(z), \tag{2.12}$$

recovering readily (2.1). The two first terms on the right-hand side of (2.12) give (2.2); the next two terms correspond physically to the work of the pressure force. The cancellation of the linear component by the Casimir is illuminating in (2.12): indeed, at leading order $p_r(z) - p_r(z_r) \sim -\rho g(z - z_r(\rho))$. To summarize, e_W is the work of the gravity force; e_{QG} and e^*_{QG} include the leading-order term of the pressure forces work; and e_a includes the exact work of pressure forces (figure 1).

2.3. *Choice of the reference stratification*

The choice of a reference stratification $\rho_r(z)$ in (2.1) is *a priori* arbitrary provided that $z_r(\rho)$ exists for any ρ value present in the fluid. Incidentally, the use of the customary horizontally averaged profile $\bar{\rho}(z)$ is not in general possible because parcels at the surface may have density less than the surface mean density $\bar{\rho}(z=0)$ (which is the minimum value for the reference stratification). However, if we want APE to be the maximal potential energy that can be extracted from a given mass field in an adiabatic way, then the reference stratification must be the so-called background stratification $\rho_b(z)$ (Lorenz 1955). It is basically the flat stratification obtained by an adiabatic rearrangement of the parcels. Therefore, a reference profile is univocally associated with any given state, though at the expense of a highly implicit function. For the case of an incompressible equation of state, this function is simply a sorting of parcels according to their densities (Winters *et al.* 1995). The background stratification ensures that the Casimirs' contributions globally vanish and that (2.3) holds. It is worth noting that other reference stratifications could be used, but then APE would lose its simple physical interpretation. For a forced-dissipative flow, the concept of background stratification still makes sense because it can be defined in terms of statistical properties of the density (cf. § 2.4) and not in terms of an adiabatic transformation.

To our knowledge, the APE definition of Holliday & McIntyre (1981) – i.e. (2.1) – has never been diagnosed in models of rotating stratified turbulence. The central goal of this paper is therefore to study the properties of (2.1) in a DNS of a turbulent flow with the choice $\rho_r(z) = \rho_b(z)$. Before that, let us further explore the properties of this background stratification.

2.4. *The background stratification*

By definition, the background stratification $\rho_b(z)$ is the density field associated with a given state $\rho(x, y, z, t)$ that minimizes the potential energy under adiabatic displacements of parcels. Under the incompressible assumption, the background stratification is also the cumulative probability density function (p.d.f.) of the density as shown below. Let us introduce the following two cumulative p.d.f.s: the volume $V(\rho)$ occupied by parcels lighter than ρ

$$V(\rho) = \int_{\rho'<\rho} \mathrm{d}V' \tag{2.13}$$

and $V(z)$, the volume of water above depth z

$$V(z) = \int_{z'>z} \mathrm{d}V'. \tag{2.14}$$

The derivatives of each of these function $\partial_\rho V$ and $\Sigma(z) = -\partial_z V$ are respectively the p.d.f. of the density weighted by the volume and the surface of the ocean at depth z. Since the function $V(z)$ is monotonic, its inverse mapping $z(V)$ exists. Composing $z(V)$ and $V(\rho)$ yields the inverse mapping of the background stratification

$$z_b(\rho) = z(V(\rho)) \tag{2.15}$$

which is the cumulative p.d.f. of the density. Using the chain rule yields

$$\frac{\partial z_b}{\partial \rho}(\rho) = -\Sigma(z)^{-1}\frac{\partial V}{\partial \rho}(\rho), \tag{2.16}$$

which is the density p.d.f. weighted by the thickness, which simplifies, in the case of a domain with a flat bottom, into

$$N_b^2(z_b(\rho)) = -\frac{g\Sigma_0}{\rho_0}[\partial_\rho V(\rho)]^{-1}, \tag{2.17}$$

where the surface $\Sigma_0 = \Sigma(z)$ is independent of z. Therefore, in practice, computing $N_b^2(z_b(\rho))$ amounts to computing the density p.d.f. $\partial_\rho V(\rho)$.

3. Model results

3.1. *Description*

Numerical simulations of a nonlinear baroclinic unstable flow in a zonal β plane channel (1000 km long and 3000 km wide, with a depth of 4000 m) centred at midlatitudes ($f = 10^{-4}$ s^{-1}) have been performed with the PE code regional ocean model system (ROMS; see details in Klein *et al.* 2008). The simulation used in this

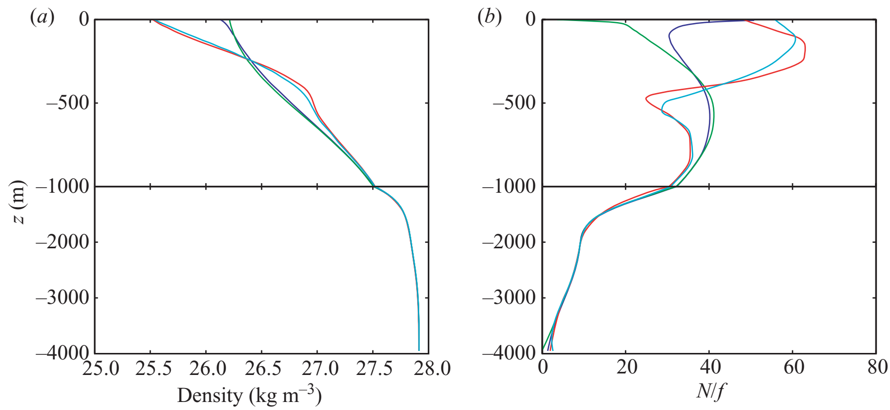

FIGURE 2. (a) Vertical profiles (with a zoomed-in view of the upper layers) of the horizontally averaged density $\bar{\rho}$ at the equilibrium (blue) and the horizontally averaged climatology density ρ_{clim} (green) and their associated background profiles ρ_b (red) and $\rho_{b_{clim}}$ (cyan). (b) N/f (dimensionless) profiles associated with the different density profiles (identified by their colour). The increase of N/f at the surface associated with $\bar{\rho}$ is evidence of the restratification process at play in this run.

paper has a 1 km horizontal resolution, corresponding roughly to $1/100°$ resolution, and 200 vertical levels concentrated at sea surface whose thickness exponentially increases with depth. The simulation, forced by a linear restoring (50 days) of its mean zonal state to a prescribed climatological state (figure 2), is integrated until the statistical equilibrium is reached (600 days from the original zonal state triggered by a small random noise). Upper-layer dynamics are further explored by Klein *et al.* (2008).

3.2. *Background stratification*

Figure 2 highlights that the horizontally averaged density profile $\bar{\rho}$ is very different from the background density profile ρ_b in the upper layers, but the two coincide in the abyss. However, when vertically integrated, these two profiles yield the same mass. Furthermore the background stratification (ρ_b) is close to the one calculated from the climatological state (ρ_b^*; figure 2). There is no physical necessity because the forcing is basically diabatic and so may modify the background stratification. This property is due to the particular choice of forcing that drives continuously the density towards the climatology value.

3.3. *Statistical properties of APE*

Because $z_r(\rho)$ is monotonic, APE density can be expressed in terms of either (z, ρ) or (z, z_b), using a composition, namely $\tilde{e}_a(z, z_r) = e_a(z, \rho_r(z_r))$, with

$$\tilde{e}_a(z, z_b) = \int_{\rho_b(z)}^{\rho_b(z_b)} (z - z_b(\rho'))g \, \mathrm{d}\rho'. \qquad (3.1)$$

The structure of APE for a fluid parcel in the parameter space (z, z_b) is sketched by the isocontours in figure 3(a). The zero contour is along the diagonal. In the vicinity of the diagonal $\tilde{e}_a(z, z_b)$ is locally quadratic in the transverse direction, which means that anharmonic effects vanish along the diagonal (figure 3b) and that APE matches the QG APE. For large vertical displacements ($|\Delta z| = |z - z_b|$) APE deviates from a harmonic potential, which is the signature of anharmonic effects.

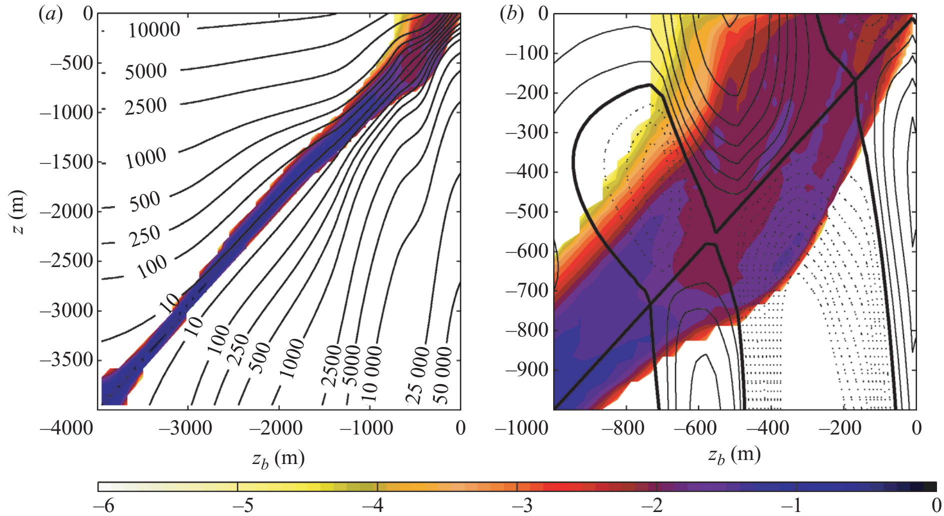

FIGURE 3. (*a*) Thin isocontours of APE $\tilde{e}_a(z, z_b)$ superimposed on the joint p.d.f. of APE (log scale in colour), expressed as functions of z and z_b. (*b*) Zoomed-in view of the upper right corner with relative importance of anharmonic effects e_{anh}/e_a (isocontours every 0.1, dashed for negative values, thick for zero value) superimposed on the same-coloured p.d.f. Isocontours are solely determined by $\rho_b(z)$, whereas colours result from the three-dimensional oceanic turbulent simulation. When looking at constant z_b (i.e. on a given isopycnal), the joint p.d.f. provides the p.d.f. of the depth z of this isopycnal: for instance the $z_b = 400$ m isopycnal spreads from roughly 800 m depth to the surface.

The joint p.d.f. of APE from the ocean turbulent eddy field (superimposed in colourscale in figure 3) has been computed by scanning every model grid cell, associating with each the pair $(z, z_b(\rho))$ and then counting the number of grid cells with a given $(z, z_b(\rho))$. We have a total of 6×10^8 grid cells in the simulation domain. Below 500 m the p.d.f. peaks around the main diagonal with a small transverse width. For upper layers, above 500 m, the p.d.f. peak deviates from the diagonal with the deviation increasing as z tends to zero. This deviation illustrates anharmonic effects in the numerical simulation due to the large Δz. These effects are important (locally 70 % of total APE) at the surface at which there are relatively dense water outcrops, corresponding to vertical displacements of up to 800 m. Interestingly, they are also important below the thermocline, at 600 m depth, where they exceed 70 % of the total APE. The sign of the anharmonic effect at 600 m depth (figure 3*b*) is directly related to the convexity of the background profile (figure 2).

3.4. *APE in the physical space*

At fixed z, APE is a functional of density only and at leading order is captured by the QG-like expression (see (2.5) or (2.6)). However, deviations from a purely QG APE are not so small (figure 4*b*) and reach 50 % at which density anomalies are large. Anharmonic effects are negative in the south part of the domain in which the vertical displacements of the isopycnals are small, and they are positive in the north part of the domain in which the vertical displacements of the isopycnals are large. This is consistent with the isocontours of figure 3(*b*) that display a small negative region in the upper right part and a positive region in the upper middle part. At a deeper level, the anharmonic effect continues to be of the same order as at the surface. It is only

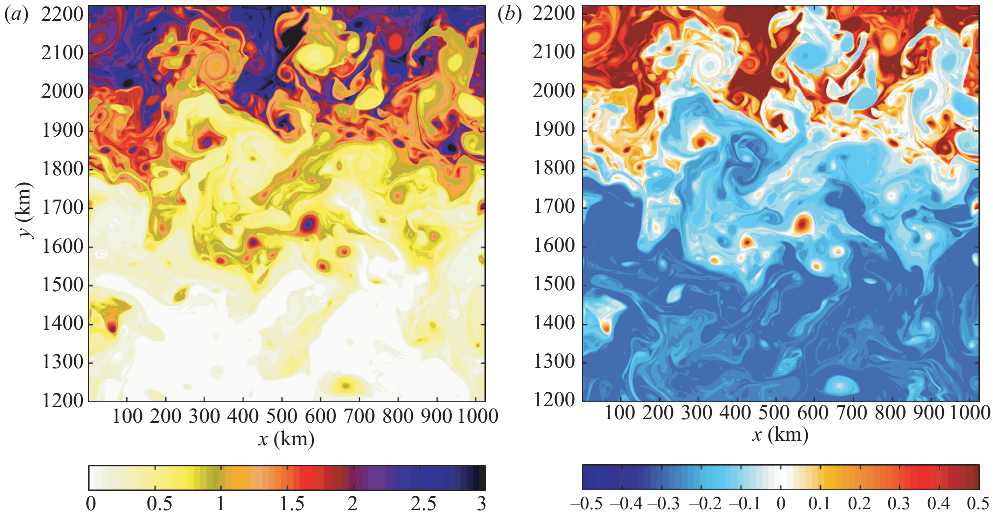

FIGURE 4. (*a*) Snapshot of the surface in the central region of the jet of APE density e_a/ρ_0 (in $m^2\ s^{-2}$). (*b*) Relative importance of anhharmonic effects e_{anh}/e_a (dimensionless) estimated from (2.1) and (2.7).

at 800 m depth that the anharmonic effect drops to a few per cent, so that APE can be considered the square of the density anomaly.

To further investigate how APE varies vertically we define an equivalent perturbation for APE density

$$\theta \widehat{=} \frac{\Delta z}{|\Delta z|}\sqrt{\frac{2e_a}{\rho_0}} \tag{3.2}$$

that can be either positive ($\Delta z > 0$) or negative ($\Delta z < 0$) and can be compared with the QG perturbation

$$\theta_{QG} = N_b(z_b(\rho))[z - z_b(\rho)]. \tag{3.3}$$

With these definitions, APE densities read $e_a = \rho_0\theta^2/2$ and $e_{QG} = \rho_0\theta_{QG}^2/2$.

On a zonal mean section, APE has nothing in common with density, though it is closely related to it. On one hand density (figure 5*a*) reflects the structure of the mass field, with classical features: a thermocline, outcropping of isopycnals, meridional gradient. On the other hand, θ reflects the primary source of energy of the flow linked to the density anomalies (figure 5*b*). Indeed, both the minimum and the maximum of θ located at depth on the southern and northern flanks of the jet are associated with Ertel potential vorticity (PV) extrema (not shown), leading to a strong meridional PV gradient that is responsible for the persistency of the baroclinic instability conditions. These extrema are sustained by a balance between the forcing feeding them and the baroclinic instability relaxing them. One interesting feature is that when the climatology contribution is subtracted from θ, the resulting field (figure 5*c*) displays chimney-like vertical structures of APE whose depth extent attains 1000 m, with a width less than 100 km. This indicates the strong impact of the mesoscale turbulence on APE.

Figure 5(*d*) reveals that APE is larger than its QG counterpart in the first 300 m below the surface (except for an area very close to the surface in the southern part

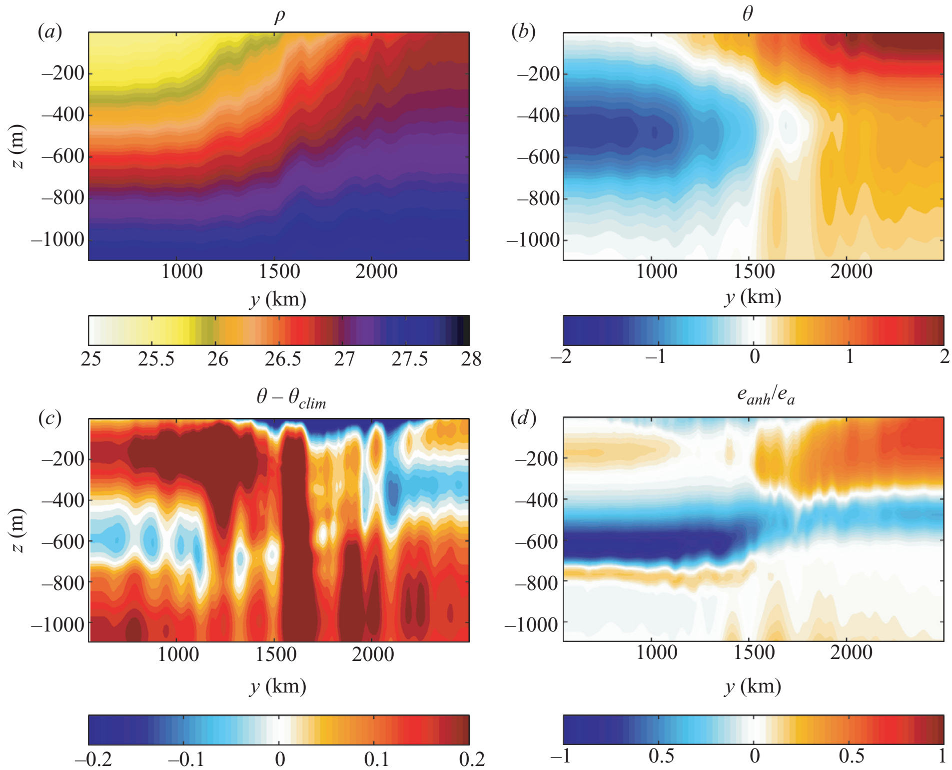

FIGURE 5. Zonal mean snapshots in the central part of the channel of (a) ρ (in kg m^{-3}), (b) θ (in m s^{-1}), (c) $\theta - \theta_{clim}$ (in m s^{-1}) and (d) e_{anh}/e_a (dimensionless).

of the domain). On the other hand it is smaller than its QG counterpart between 300 m and 700 m. Again these positive and negative deviations of APE from its QG expression, which attain more than 50 %, are consistent with the isocontours of figure 3(b) that display, on the average, a positive value above 300 m and a negative value between 300 m and 700 m. This means that the amplitude and sign of these anharmonics effects are entirely determined by the background density profile and mostly by its curvature as discussed in § 2.1.

3.5. *APE in the spectral space*

The definition of θ proposed in (3.2) also allows the computation of the APE spectra at different depths:

$$e_a(k, z) = \frac{1}{2}\int_0^{2\pi} |\widehat{\theta}|^2 k \, \mathrm{d}\varphi, \tag{3.4}$$

where $\widehat{\theta}(k, \varphi, z)$ is the horizontal Fourier transform of $\theta(x, y, z)$ in polar coordinates. Figure 6(a) shows the distribution of APE in a spectral space. For a given horizontal scale, the maximum of APE is at the surface, because of the surface-intensified nature of the turbulence. APE at sub-mesoscale ($k > 50$) is also intensified at the surface but decreases rapidly with depth. More precisely, in the upper 100 m, APE isocontours are straight and inclined, indicating that the decay of APE is exponential (because the vertical scale is a log scale). This exponential decay of surface dynamics is well captured by the surface quasi-geostrophic (SQG) theory. A small exponential decay

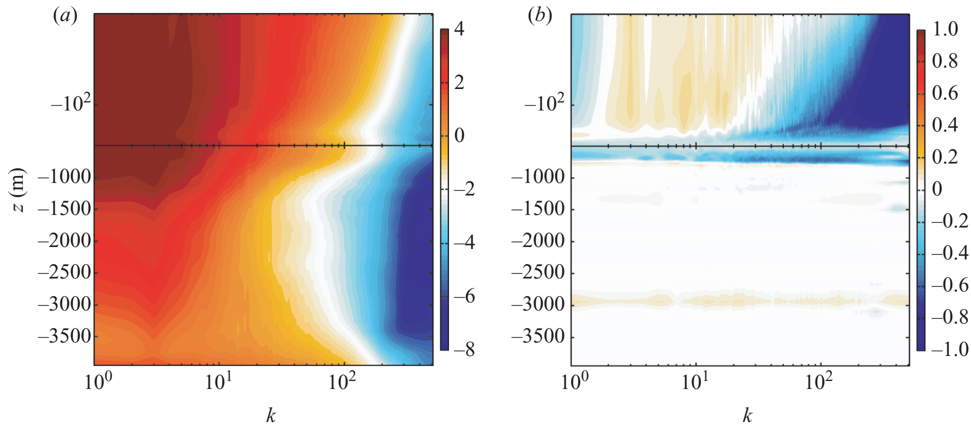

FIGURE 6. (a) APE horizontal spectrum (isocontours of $\log_{10}\widehat{\theta}^2$) as a function of depth. Upper 500 m are in log scale in order to emphasize the vertical exponential decay near the surface. (b) Similar to (a) but for the ratio of QG APE and APE (isocontours of $\log_{10}(\widehat{\theta}^2/\widehat{\theta}^2_{QG})$.

is also present at the bottom due to the bottom-trapped dynamics analogous to the SQG dynamics. Below the thermocline, APE decreases rapidly with k, indicating a QG regime. These results are in accordance with the results of Klein *et al.* (2008) that reveal a k^{-2} spectrum slope for the density near the surface instead of a $k^{-4.5}$ spectrum slope in the abyss.

The anharmonic effects have a relatively simple structure in the (k, z) space (figure 6b). They are mostly negative for large k and positive for smaller k in the upper layers. Again this is consistent with the isocontours of figure 3(b). Indeed, the Burger number being close to one in this simulation (Klein *et al.* 2008), small horizontal structures also have a small vertical extent, allowing only small vertical displacements of the isopycnals. The opposite is true for the larger scale structures. Figure 3(b), on the other hand, reveals that anharmonic effects in the upper 300 m are negative in the upper right part in which small displacements of the isopycnals are allowed and positive in the middle part in which large displacements of the isopycnals are allowed. Below the thermocline, QG APE is too large; i.e. anharmomic effects are negative, at all scales. Below 1000 m, anharmonic effects are negligible.

4. Conclusion

We have confirmed that APE density as defined by Holliday & McIntyre (1981) takes into account terms that are missing from the basic and the QG definition of APE given by Pedlosky (1987). As such it is the more appropriate within the framework of the primitive equations. This remains true even when the hydrostatic assumption is relaxed. Like every APE, it is based on the reference density profile. We have shown that not every profile suits APE. Following Lorenz's (1955) physical interpretation of APE, we used the background density profile obtained by an adiabatic rearrangement of the parcels. We have shown that for an incompressible equation of state, this profile is the cumulative p.d.f. of density. This property allows the computation of the background stratification in a more complex geometry. Using these results we have estimated APE density in a DNS of a rotating stratified turbulent flow that uses a PE model. To our knowledge, such an estimation in a PE simulation has never been done before. The estimated APE density significantly departs from its QG counterpart because of the strong isopycnal displacements. But it is essentially the curvature of the background density profile that determines the amplitude and the sign of the departure of APE from its QG counterpart, known as anharmonic effects. These anharmonic effects are significant principally within the upper oceanic layers.

REFERENCES

Bannon, P. R. 2003 Hamiltonian description of idealized binary geophysical fluids. *J. Atmos. Sci.* **60**, 2809–2819.

Charney, J. G. 1971 Geostrophic turbulence. *J. Atmos. Sci.* **28**, 1087–1095.

Holliday, D. & McIntyre, M. E. 1981 On potential energy density in an incompressible stratified fluid. *J. Fluid Mech.* **107**, 221–225.

Hua, B. L. & Haidvogel, D. B. 1986 Numerical simulations of the vertical structure of quasi-geostrophic turbulence. *J. Atmos. Sci.* **43**, 2923–2936.

Klein, P., Hua, B. L., Lapeyre, G., Capet, X., Le Gentil, S. & Sasaki, H. 2008. Upper ocean turbulence from high 3-d resolution simulations. *J. Phys. Oceanogr.* **38**, 1748–1763.

Lorenz, E. N. 1955 Available potential energy and the maintenance of the general circulation. *Tellus* **7**, 157–167.

McWilliams, J. C. 1989 Statistical properties of decaying geostrophic turbulence. *J. Fluid Mech.* **198**, 199–230.

Morrison, P. J. 1998 Hamiltonian description of the ideal fluid. *Rev. Mod. Phys.* **70**, 467–521.

Pedlosky, J. 1987 *Geophysical Fluid Dynamics*. Springer.

Shepherd, T. G. 1993 A unified theory of available potential energy. *Atmos. Ocean* **31**, 1–26.

Winters, K. B., Lombard, P. N., Riley, J. J. & D'Asaro, E. A. 1995 Available potential energy and mixing in density-stratified fluids. *J. Fluid Mech.* **289**, 115–128.